Incorporating seismic interferometry and full waveform inversion

Jinji Li* and Kristopher A. Innanen
li.jinji@ucalgary.ca

ABSTRACT

Seismic interferometry, through the cross-correlation of data recorded by receiver pairs, can extract Green's function, enabling the potential redatuming of signals using passive datasets. This capability holds promise for integration with full waveform inversion (FWI) to continuously update subsurface property estimates in real time. This report presents a preliminary investigation into the feasibility of combining seismic interferometry and FWI by introducing a novel objective function aimed at mitigating interference patterns in seismic waveforms. A straightforward numerical example demonstrates that, under conventional surface acquisition constraints, seismic interferometry can enhance the estimation of P-wave velocity. However, further comprehensive research is needed to assess the algorithm's performance across diverse scenarios, including elastic applications.

SHOWCASE of SEISMIC INTERFEROMETRY

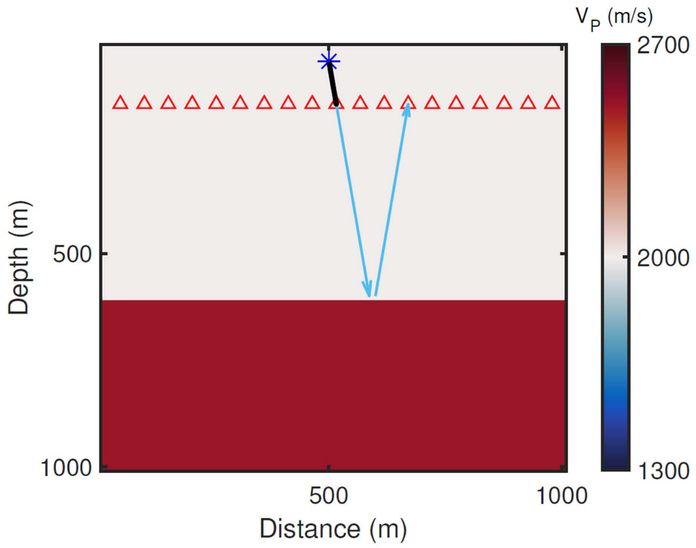

Figure 1. 2-layered velocity model and schematic acquisition.

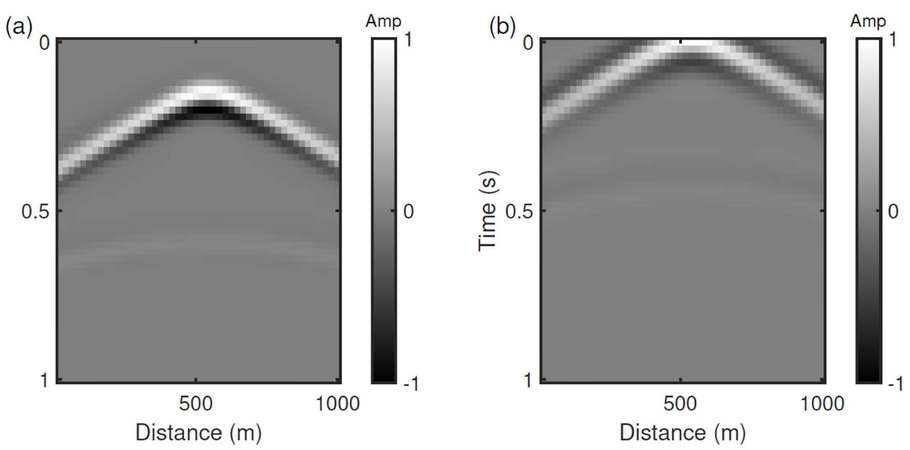

Figure 2. Shot gathers. (a) Original shot gather. (b) Redatumed shot gather with virtual source in the middle receiver.

SI-FWI FORMULATION

$$min_{\boldsymbol{p}}\phi(\boldsymbol{p}) = \frac{1}{2}\left\|Ru(Ru)^{\dagger} - C_0\right\|_2^2, \quad (1)$$

s.t. $Su = f$.

$$C_0 = dd^{\dagger}. \quad (2)$$

It is important to note that this problem is subject to the wave equation, which might utilize the original source vector to perform passive FWI through arbitrary excitations. The adjoint wavefield $\bar{k}$ and gradient $\boldsymbol{g}$ with respect to model parameter can be represented:

$$\bar{k} = 2R^T[R\bar{u}R\bar{u}^{\dagger} - C_0]R\bar{u}. \quad (3)$$

$$\boldsymbol{g} = \left\langle \frac{\partial s}{\partial \boldsymbol{m}}\bar{u}, \bar{k} \right\rangle. \quad (4)$$

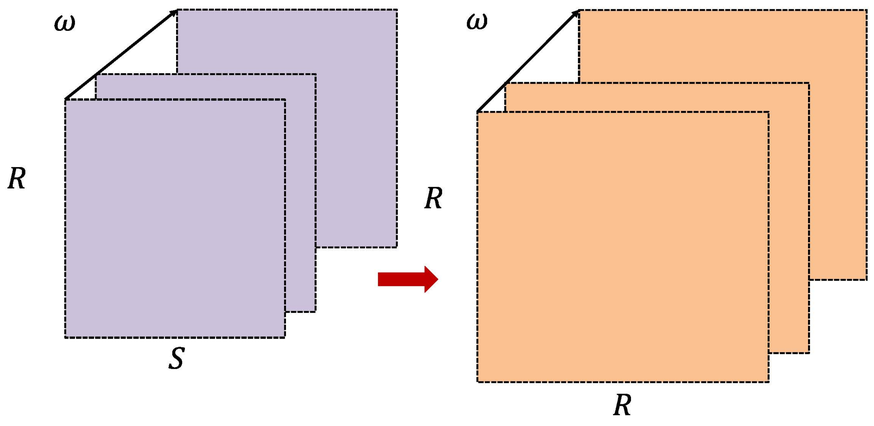

Figure 3. Frequency domain SI-FWI ideas. Using seismic interferometry transforms the data with sparse source acquisition to a denser acquisition with virtual sources.

RESULTS

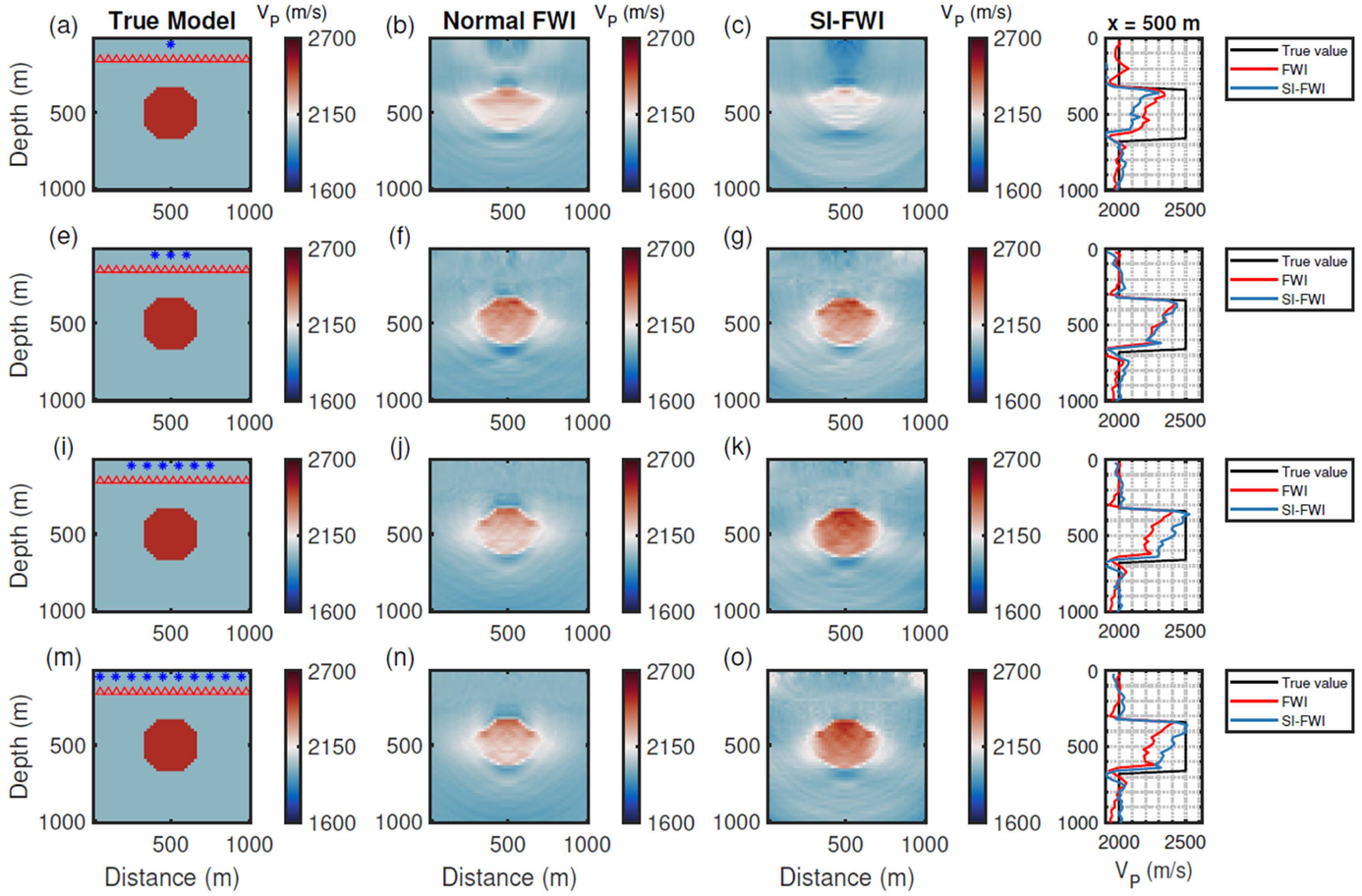

Figure 4. SI-FWI tests. The first column ((a), (e), (i), (m)) shows the true model and acquisitions with various source number. The second column ((b), (f), (j), (n)) shows the results of conventional FWI. The third column ((c), (g), (k), (o)) shows SI-FWI results. The last column shows the vertical profile at x = 500 m, with the black lines from the true model, the red lines from the conventional FWI, and the light blue lines from the SI-FWI.

ACKNOWLEDGEMENTS

This work was funded by CREWES industrial sponsors and NSERC (Natural Science and Engineering Research Council of Canada) through the grant CRDPJ 543578-19. One of the authors of this report was supported by the CSEG Foundation.

NSERC CRSNG
UNIVERSITY OF CALGARY
FACULTY OF SCIENCE
Department of Earth, Energy, and Environment